Dances with Anthrax: Wolves (Canis lupus) Kill Anthrax Bacteremic Plains Bison (Bison bison bison) in Southwestern Montana

Article *in* Journal of Wildlife Diseases · January 2014

DOI: 10.7589/2013-08-204 · Source: PubMed

5 authors, including:

Jason K. Blackburn
University of Florida
217 PUBLICATIONS **3,923** CITATIONS

SEE PROFILE

Kathleen A Alexander
Virginia Tech
141 PUBLICATIONS **3,421** CITATIONS

SEE PROFILE

DOI: 10.7589/2014-06-157 *Journal of Wildlife Diseases*, 51(2), 2015, pp. 318–331

MODELING THE ENVIRONMENTAL GROWTH OF *PSEUDOGYMNOASCUS DESTRUCTANS* AND ITS IMPACT ON THE WHITE-NOSE SYNDROME EPIDEMIC

Hannah T. Reynolds,[1] Tom Ingersoll,[2] and Hazel A. Barton[1,3]

[1] Department of Biology, University of Akron, 185 E. Mill St., Akron, Ohio 44325, USA
[2] National Institute for Mathematical and Biological Synthesis, 1122 Volunteer Blvd., Suite 106, University of Tennessee, Knoxville, Tennessee 37996, USA
[3] Corresponding author (email: bartonh@uakron.edu)

ABSTRACT: White-nose syndrome (WNS) has had a devastating effect on North American bat populations. The causal agent of WNS is the fungal pathogen, *Pseudogymnoascus destructans* (*Pd*), which has been shown to persist in caves after the eradication of host populations. As nonpathogenic *Pseudogymnoascus* spp. display saprophytic growth and are among the most commonly isolated fungi from caves, we examined whether *Pd* could grow in cave sediments and the contribution such growth could have to WNS disease progression. We inoculated a range of diverse cave sediments and demonstrated the growth of *Pd* in all sediments tested. These data indicate that environmental growth of *Pd* could lead to the accumulation of spores above the estimated infection threshold for WNS, allowing environment-to-bat infection. The obtained growth parameters were then used in a susceptible-infected-susceptible mathematic model to determine the possible contribution of environmental *Pd* growth to WNS disease progression in a colony of little brown bats (*Myotis lucifugus*). This model suggests that the environmental growth of *Pd* would increase WNS infection rates, particularly in colonies experiencing longer hibernation periods or in hibernacula with high levels of organic detritus. The model also suggests that once introduced, environmental *Pd* growth would allow the persistence of this pathogen within infected hibernacula for decades, greatly compromising the success of bat reintroduction strategies. Together these data suggest that *Pd* is not reliant on its host for survival and is capable of environmental growth and amplification that could contribute to the rapid progression and long-term persistence of WNS in the hibernacula of threatened North American bats.

Key words: Bat populations, cave fungi, disease model, environmental growth, extirpation, *Pseudogymnoascus destructans*, white-nose syndrome.

INTRODUCTION

Pathogens play an important role in the structure and population size of their animal hosts. Directly transmitted pathogens either enter a persistent equilibrium with their host, or they are eliminated by host resistance or as the host population density falls below a threshold necessary for continued transmission (Anderson and May 1981; Anderson 1991). While only 4% of current global species decline is due to infectious disease, disproportionately high numbers (65%) are due to emerging infectious mycoses, such as the amphibian pathogen *Batrachochytrium dendrobatidis* (Fisher et al. 2012). Some fungal pathogens, such as the human pathogen *Histoplasma capsulatum*, can live as free-living saprotrophs (Maresca and Kobayashi 1989). However, the dimorphic nature of *H. capsulatum* restricts it to a yeast-like stage in a living host, preventing host-to-host transmission; infections are caused solely by environmental exposure. Nonetheless, if a fungal pathogen could spread both through contact transmission and grow in the environment, it could cause an epidemic influenced by both host interactions and environmental exposure. Uncoupled from the pathogen-host density relationship and the necessity to maintain a threshold host population, such a pathogen could quickly drive its host species to extinction (Godfray et al. 1999; de Castro and Bolker 2005; Mitchell et al. 2008; Fisher et al. 2012).

In this paper, we explore the role that environmental propagation could have in the disease ecology of *Pseudogymnoascus*

(= *Geomyces*) *destructans* (*Pd*), the causative agent of white-nose syndrome (WNS) in bats (Gargas et al. 2009; Lorch et al. 2011; Minnis and Lindner 2013). First identified in New York State in 2006, WNS has rapidly spread across the northeastern US, infecting numerous cave- and mine-hibernating bat species, including *Myotis lucifugus*, *Myotis sodalis*, *Myotis grisescens*, *Myotis septentrionalis*, *Eptesicus fuscus*, and *Perimyotis subflavus*, which have experienced variable, but significant declines from WNS. Average declines of 91% are seen across a five-state region for the once-ubiquitous little brown bat (*M. lucifugus*) (Turner et al. 2011). Indeed, colony declines are so dramatic that *M. lucifugus* may be regionally extirpated by 2020 (Frick et al. 2010a).

The potential for saprophytic growth of *Pd* comes from several lines of evidence, including its growth on multiple substrates (Verant et al. 2012; Raudabaugh and Miller 2013; Smyth et al. 2013), production of numerous saprotrophic enzymes (Raudabaugh and Miller 2013; Reynolds and Barton 2014), and presence of *Pseudogymnoascus* spp. as common members of the cave fungal biome (Johnson et al. 2013; Vanderwolf et al. 2013). Environmental growth would have important implications for WNS disease management, increasing the risk of human-mediated spread and complicating efforts to reintroduce extirpated bat species. While the presence of *Pd* in the sediments of infected hibernacula has been confirmed in the absence of bats (Lindner et al. 2011; Lorch et al. 2013a, b), no distinction has been made between the presence of spores shed by infected bats and the propagation of the fungus within the environment. In this paper, we directly measured the rates of *Pd* growth in cave sediments and used these data as parameters within a mathematic model of WNS disease ecology. This model predicts how the environmental growth of *Pd* could affect bat colony stability in the face of the WNS epidemic.

MATERIALS AND METHODS

Geochemical analysis

Calcite Quarter Cave, Kentucky, contains a small colony of hibernating bats and was outside of the WNS endemic zone at the time of our study (January 2011). Sediments tested were chosen to represent a number of different geochemical niches, including silica-rich muds produced as a result of speleogenesis (mud-crack clay), silicate-rich sands from the dissolution of a sandstone cap rock (entrance sand) or introduced by an infiltrating vadose stream (stream sand, stream silt/gravel), and sediments rich in surface-derived organic material from flood events (flood debris). Ten subsamples of each sediment were used for geochemical analysis using scanning electron microscopy energy-dispersive spectroscopy (SEM-EDAX), and one subsample of each sediment was analyzed for the ratio of carbon to hydrogen, oxygen, and nitrogen, with total organic carbon (TOC) being differentiated by combustion and thermal-optical analysis (Elemental Analysis Inc., Lexington, Kentucky, USA; see Supplementary Material in the Supplemental Methods section for further detail).

Strains and growth conditions

Pseudogymnoascus destructans MYA-4855 (stored as *Geomyces destructans*), *Pseudogymnoascus* sp. ATCC 16222 (*P.* sp.; stored as *Geomyces pannorum* var. *pannorum*), and *Penicillium pinophilum* MYA-9644 (*Pen. p.*) were obtained from the American Type Culture Collection (Manassas, Virginia, USA) and cultured at 10 C on potato dextrose agar before harvesting, as described by Shelley et al. (2013). Sediments were sterilized, dried, and rewetted to their original moisture content with sterile, deionized water, and 1×10^4 conidia were added to each gram of sediment (see Supplemental Methods section in the Supplementary Material). Samples were incubated at 10 C and 95% humidity in a KB024 environmental chamber (Darwin Chambers Co., St. Louis, Missouri, USA). Dilution-to-extinction plating of 0.1 g of inoculated sample was used to measure viable fungal colony-forming units (CFUs). All fungi were quantified on days 0, 14, 28, and 56, while *Pd* was further examined for viability on day 238. The exponential growth rates for *Pd* and *P.* sp. were calculated using the *lm* function in R version 2.15 (R Development Core Team 2012) from the average increase in CFUs between days 0 and 14, while *Pen. p.* was calculated from the increase between days 14 and 28. The

TABLE 1. Empirical geochemical and calculated *Pseudogymnoascus destructans* ecology parameters determined in this study.[a]

	Geochemistry (% weight)										
	Al	Ca	Fe	O	P	Si	C:N	TOC (mg/g)	β_{xr} (CFU/d)	K_z (total CFU/g)	μ_{Pd} (log CFU/d)
Stream sand	1.74	0.12	1.05	30.72	0.14	13.16	1:1	0.54	0.046	1.30×10^4	−0.004
Stream gravel	3.12	0.18	2.93	35.44	0.05	11.6	4:1	2.27	0.202	1.30×10^4	−0.007
Entrance sand	5.52	0.5	2.5	42.22	0.08	19.4	5:1	5.55	0.215	5.64×10^4	−0.003
Clay	6.67	0.51	2.85	43.4	0.08	27.24	7:1	9.90	0.307	2.47×10^5	−0.008
Flood debris	1.43	1.46	0.5	31.49	0.08	6.57	30:1	135.11	0.421	3.57×10^6	−0.003

[a] Al = aluminum; Ca = calcium; Fe = iron; O = oxygen; P = phosphorus; Si = silicon; C:N = carbon to nitrogen ratio; TOC = total organic carbon; CFU = colony-forming units.

sediment carrying capacities were estimated from the average number of CFUs at day 28. Regression analysis for carrying capacity against various parameters was performed using the *lm* function in R.

RESULTS

To determine if the growth of *Pd* is possible within hibernacula, we inoculated *Pd* conidia into five diverse cave sediments that were geochemically defined prior to analysis (Table 1). The TOC ranged from 0.54 mg/g in stream sand to 135.11 mg/g in flood debris. The high carbon-to-nitrogen (C:N) ratio in the flood debris suggests that it had been composting in the cave for several years (C:N ratio 30:1), while the other sediments demonstrated C:N levels similar to those of an oligotrophic cave environment in an agricultural setting (C:N ratio 1–7:1; Table 1) (Boyer and Pasquarell 1996). We used SEM-EDAX to quantify the major elements in these sediments, and we assessed the overall sediment geochemical composition using principal component analysis (Fig. 1). The greatest difference in sample geochemistry was determined by the availability of carbon, followed by the presence of silica and oxygen (presumably due to the presence/absence of silicate sands; 98.5% observed variance) (Fig. 1 and Table 1). Along with the known saprotrophic species tested, *Pd* grew in all the sediments, including the lowest-nutrient sediment (0.54 mg/g TOC) (Fig. 2). Significant amplification of the pathogen was observed in flood debris, with a 1,000-fold increase in CFUs (Fig. 2).

We observed the continued growth of *Pd* in the flood debris after 56 d, with maximal growth at 28 d in others (Fig. 2). To determine the sediment-specific carrying capacities of *Pd* (K_z), we examined the amount of fungal material after 28 d of growth (Fig. 2 and Table 1). A linear regression of growth capacity versus TOC indicated that the *P.* sp. and *Pen. p.* have similar carrying capacities at the lower nutrient levels (Fig. 3), while *Pd* had the lowest amplification per mg of TOC among the fungi tested across a range of nutrient concentrations (Fig. 3 and Table 1). Correlation analysis against the various constituents of the sediments revealed that the C:N ratio had the highest correlation with carrying capacity (K_z, Pearson's $r>0.995$), followed by TOC (Pearson's $r>0.992$); these two parameters were strongly co-correlated (Pearson's $r>0.992$).

The loss of *Pd* CFUs at 56 d did not directly correlate with the amount of TOC available, with a greater loss of *Pd* in the clay (9.90 mg/g TOC) versus entrance sand (5.55 mg/g TOC) (Fig. 2), suggesting that *Pd* persistence may be affected by other geochemical factors not defined here (e.g., water availability, type of organic carbon). To determine the extent to which *Pd* is lost over the summer when the bats are absent, we examined *Pd* levels in the sediments after ~8 mo (238 d; Fig. 2). These data demonstrate that while

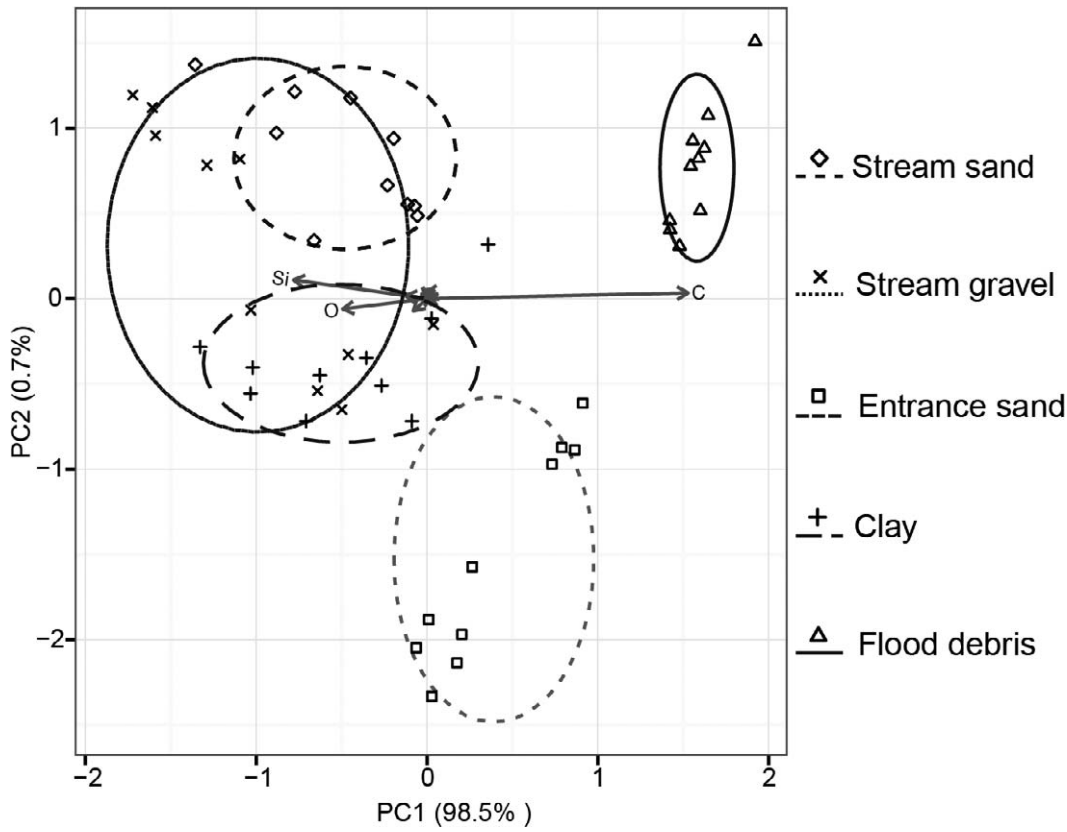

FIGURE 1. Principal component analysis of hibernacula sediments. The values used come from 10 energy dispersive X-ray spectroscopy scans for each of five cave sediment samples collected in January 2011, and include 16 primary geochemical elements. The ellipses show 95% confidence intervals for placement of each sediment type. Si=silicon; O=oxygen; C=carbon; PC1=principal component 1; PC2=principal component 2.

Pd can subsist in these sediments for an extended period without organic carbon supplementation, there is some loss of viability (Fig. 2).

Using these data, estimated sediment-specific parameters for *Pd* growth dynamics, including growth rate (β_{xr}), carrying capacity (K_z), and seasonal decline of *Pd* in the absence of bats (μ_{Pd}), were used in a two-component, susceptible-infected-susceptible (SIS) model (Fig. 4 and Table 1). This model was used to examine bat colony survival under five scenarios: exposure to WNS in a range of hibernation seasons, persistence or elimination of *Pd* in bats through the summer, introduction of WNS through fomites or infected bats, propagation of *Pd* in type of sediment, and the unrestricted or suppressed environmental growth of *Pd* (Fig. 5).

The model

Our SIS model consisted of difference equations, with a time step of 1 d, to assess host infection rate and persistence when challenged by an environmental reservoir of *Pd* (in sediments providing varying growth rate and carrying capacity; Table 1 and Fig. 4). We used *M. lucifugus* as a model bat species due to the wide availability of population data for modeling. We modeled a closed colony, with no outside migration, hibernating in a cave chamber with volume $V_H=1{,}000$ m^3 and sediment of mass $M=10^6$ g. To determine whether a sufficient number of spores

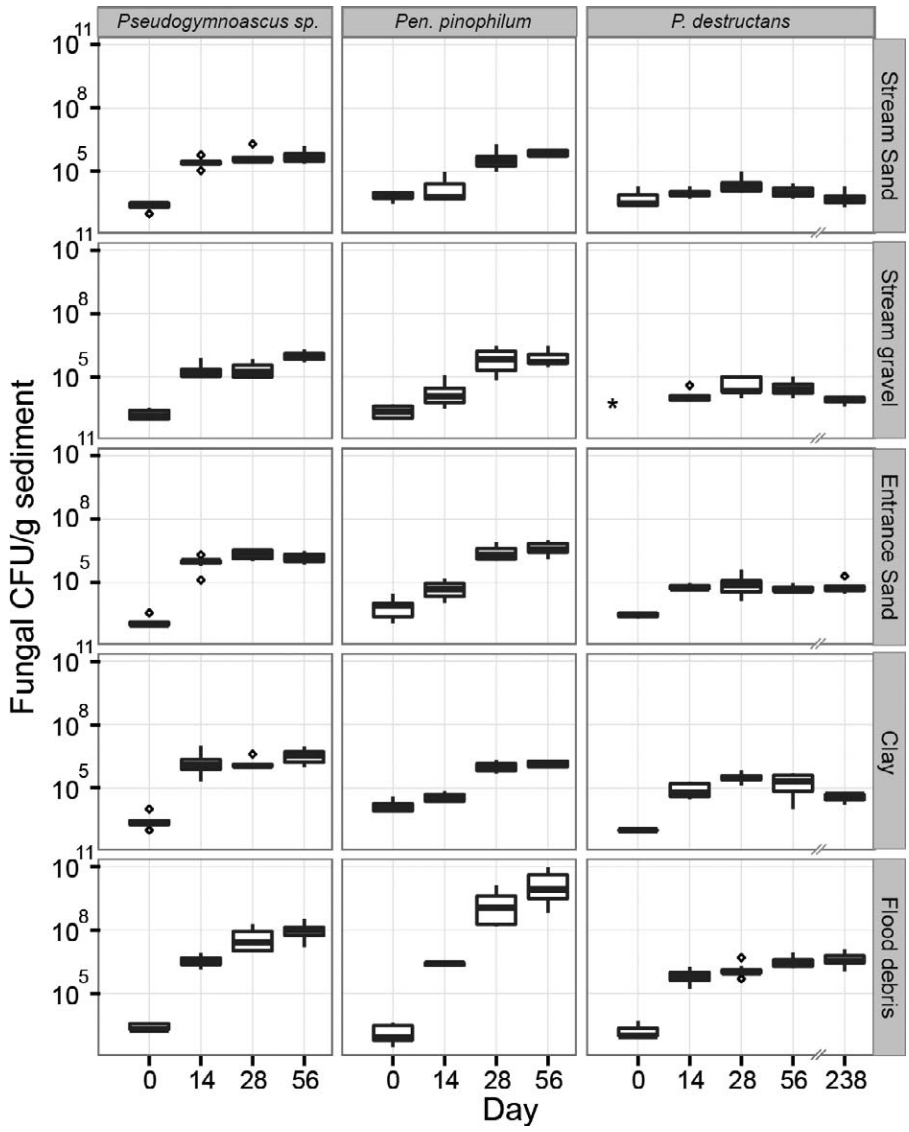

FIGURE 2. Fungal growth. The increase in fungal growth was determined by an increase in colony-forming units (CFU)/g of sediment over time. The boxplot boundaries indicate the first and third quartiles, with the mean as the centerline, whiskers as 1.5× the interquartile distance, and outliers plotted as diamonds. The asterisk indicates the original inoculation of 1×10^4 conidia per gram of sediment. *Pseudogymnoascus* sp.=*Pseudogymnoascus* sp. ATCC 16222; *Pen. pinophilum*=*Penicillium pinophilum* ATCC MYA-9644; *P. destructans*=*Pseudogymnoascus destructans* ATCC MYA-4855.

could accumulate in the atmosphere around bats, an individual was modeled as a sphere with a diameter of 87 mm (Leconte 1831), giving a volume of $V_b \approx 0.000345$ m^3 per bat. The infectious dose used ($\theta = 10^6$ CFU per bat) was extrapolated from the data of Lorch et al. (2011). Their study was performed on a small number of captive bats and was not designed to establish disease ecology parameters, but rather to demonstrate the role of *Pd* in WNS. Nonetheless, it provided the most reliable data on timing and mortality to estimate parameters that

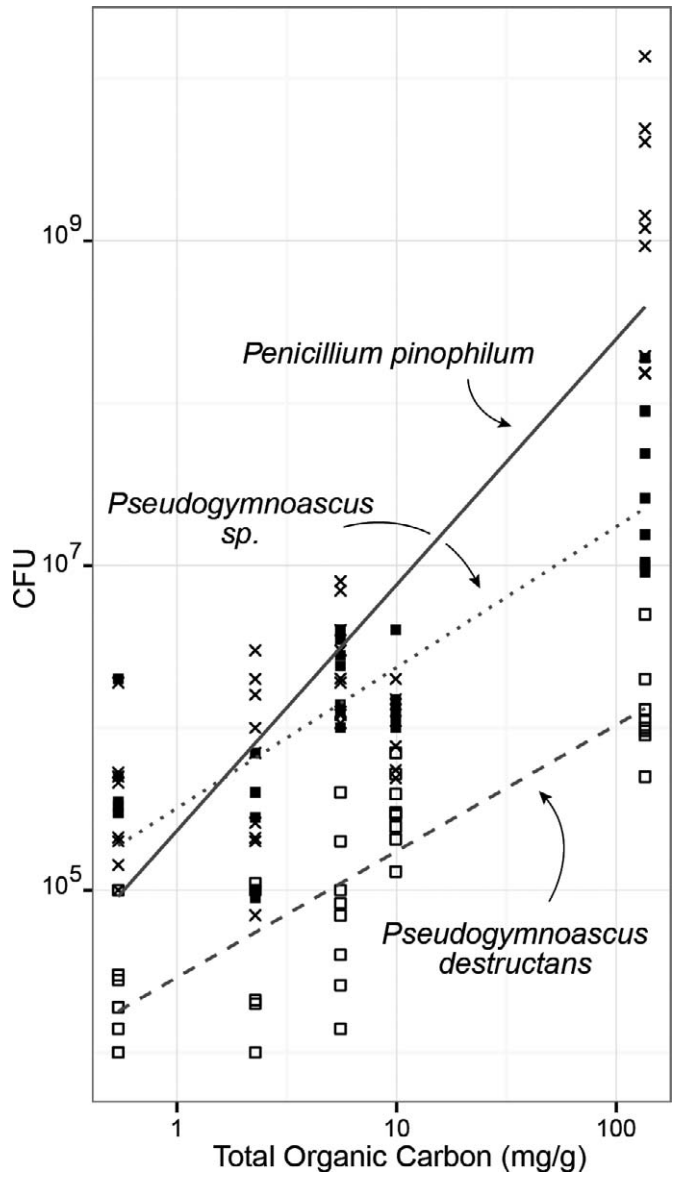

FIGURE 3. Fungal growth under different organic carbon scenarios. The increase in colony-forming units (CFU) for each species over 28 d is shown for the amount of organic carbon (mg/g) in each sediment and plotted in semilog form with a simple linear regression.

may apply to WNS in natural settings. We note that the infection parameters (infectious dose, shed rate, incubation period, and mortality rate) are accordingly uncertain. During hibernation, infected bats (Y) became infectious (Y_{inf}, a subset of Y) following a 20-d incubation period τ_I and died with an experimental WNS-related mortality rate ρ_b of 0.98% per day after a 120-d incubation period τ_M (Lorch et al. 2011):

$$\text{for } t=1-H: Y_{\text{inf}_t}=Y_{t-\tau I}-\rho_b Y_{t-\tau I-\tau M} \quad (1)$$

Susceptible bats (X) became infected through frequency-dependent bat-to-bat

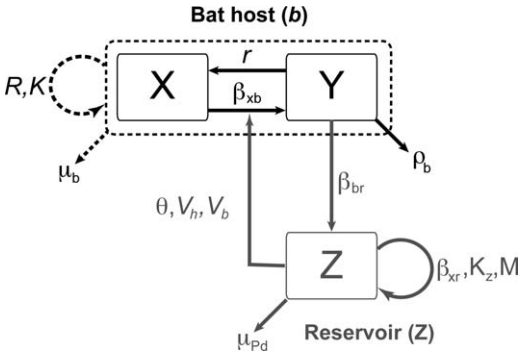

FIGURE 4. The susceptible-infected-susceptible model. Within specific hibernacula, the bats are represented by a susceptible (X) and infected (Y) population. For simplification (and using empirical data), we assume that the elimination rate of *Pseudogymnoascus destructans* (*Pd*) from bats during hibernation is zero, with bats lost from the infected compartment through natural and white-nose syndrome-associated mortality (ρ_b). Susceptible bats become infected through bat-to-bat infection via a density-dependent transmission rate (β_{xb}), and they shed *Pd* spores into the environment at a rate of β_{br}. Bats can also be infected from spores in the environment based on the environmental spore density, bat size, and infection dose ($V_bZ_t/\theta\times V_h$). In each sediment, the rate of fungal amplification (β_{xr}), carrying capacity (K_z), and spore loss (μ_{Pd}) has been calculated from empirical data within this study (Table 1; for additional parameters, see Supplementary Table 1).

transmission with an infection rate (β_{xb}) of one bat per infected bat per day. This estimate is based on the proximity and frequent movement of hibernating bats and empirical observations of high bat-to-bat infection (Lorch et al. 2011). Environment-to-bat transmission dynamics were based on the density of environmental spores and the establishment of an environmental infectious dose. The colony dynamics of susceptible and infected bats were modeled using frequency-dependent (Keeling and Rohani 2008) logistic equations:

$$\text{for } t=1-H: X_{t+1} = X_t - \beta_{xb} Y_{\inf_t}\left(\frac{X_t}{X_t+Y_t}\right) - \frac{V_b X_t Z_t}{\theta * V_H} - \mu_b X_t \quad (2)$$

$$Y_{t+1} = Y_t + \beta_{xb} Y_{\inf_t}\left(\frac{X_t}{X_t+Y_t}\right) + \frac{V_b X_t Z_t}{\theta * V_H} - \rho_b Y_{(t-\tau I-\tau M)} - \mu_b Y_t \quad (3)$$

where X_t and Y_t are the susceptible and infected bats at time t, respectively (initial values: X_0=9,000 bats, Y_0=0 or 1 bat), μ_b is the background bat mortality rate calculated from the average of the *M. lucifugus* male and female yearly survival (0.0032 bats/d) (Keen and Hitchcock 1980), and Z_t is the number of *Pd* CFUs at time t (initial value: Z_0=0 or 1 CFU). For simplification, we assumed an equal male to female ratio, equal susceptibility to WNS, equal fecundity of surviving bats, and that WNS transmission, mortality, and *Pd* shedding occur only during hibernation. We further assumed that the probability of infection was 1 when the spore encounter rate met the infection threshold and 0 when it was below this threshold. While it is established that surviving bats can heal from the disease ex situ (Meteyer et al. 2011), it is unknown whether *Pd* can persist on bats through the summer at levels below the PCR detection limit (Meteyer et al. 2009, 2011). We therefore simulated WNS with and without spore persistence in infected bats and used the bat recovery rate r = 0.1 or 0 bats/d (for full elimination or persistence of *Pd*, respectively) during the summer season:

$$\text{for } H<t<365 \text{ and } t\neq 250: X_{t+1} = X_t + rY_t - \mu_b X_t \quad (4)$$

$$\text{for } H<t<365: Y_{t+1} = Y_t - rY_t - \mu_b Y_t \quad (5)$$

To model reproductive dynamics, we assumed that all surviving females gave birth to susceptible offspring on the same arbitrarily selected day in early June (250 d after the start of hibernation; Krochmal and Sparks 2007; Frick et al 2010b):

$$\text{for } t=250: X_{t+1} = X_t + 0.5R(X_t+Y_t)\left(1-\frac{X_t+Y_t}{K}\right) - \mu_b X_t \quad (6)$$

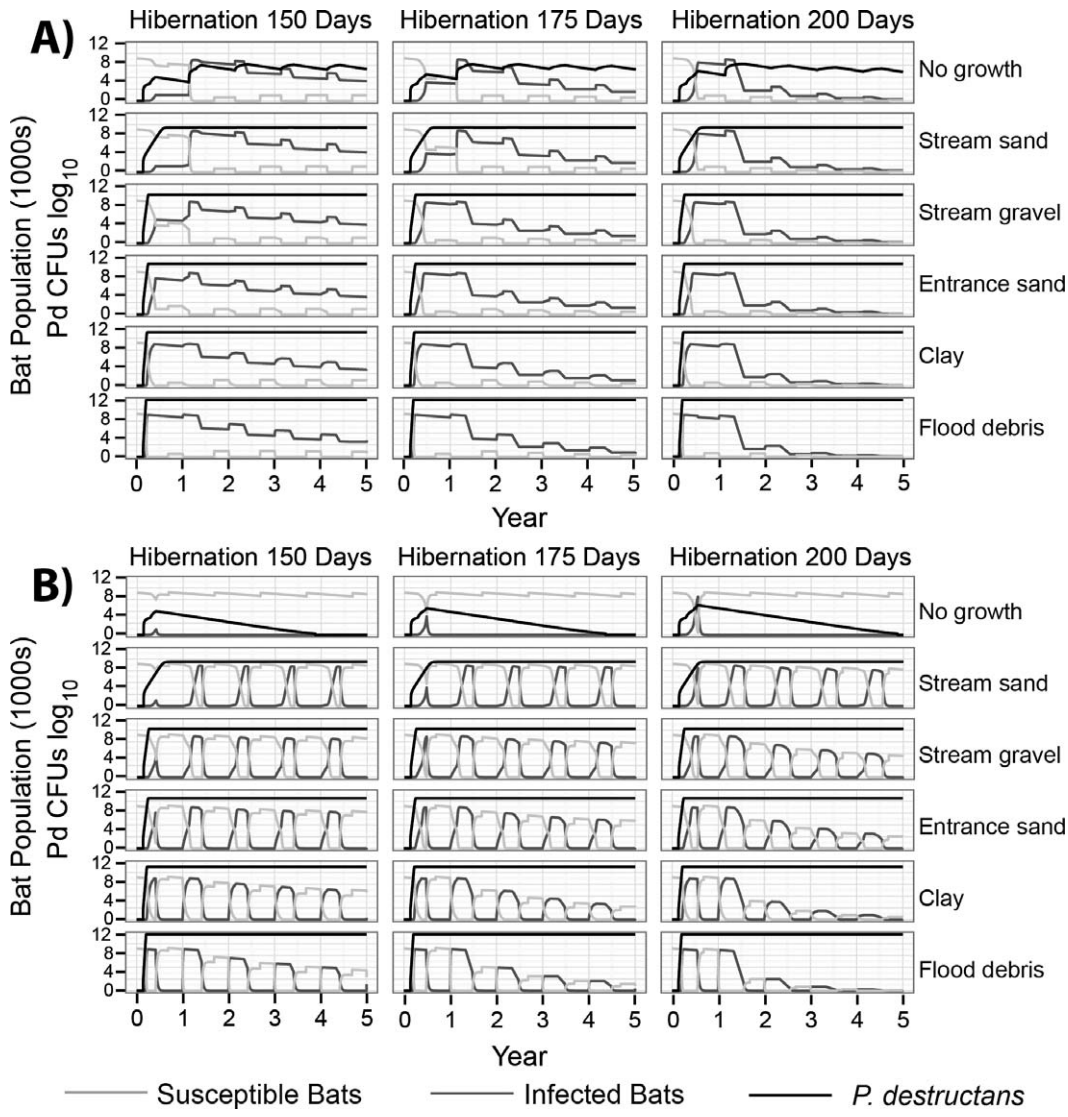

FIGURE 5. The influence of environmental *Pseudogymnoascus destructans* (*Pd*) growth on white-nose syndrome disease outcome and colony extirpation. We examined the effect of hibernation length on extirpation of 9,000 bats in the model hibernaculum. Simulations tracking susceptible and infected bats and *Pd* colony-forming units (CFUs) were run for 5 yr in each sediment type, beginning on day 0 of the hibernation season, sampling daily, with hibernation ending after 150, 175, and 200 d. Infected bats become infectious after 20 d and die after 102 d of infection. (A) Disease progression is initiated by the introduction of a single bat, and *Pd* spores can persist on bats through the summer. (B) Disease progression is initiated by the introduction of a single bat, and *Pd* is eliminated from bats in the summer. The saw-like pattern seen within this bat colony represents the return of all the bats to the susceptible population on day 0 of hibernation.

where R is the yearly female reproductive rate (0.95) taken from the average fecundity for *M. lucifugus* (Frick et al. 2010b), and K is the carrying capacity for bat colony size in this hypothetical system (10,000 bats). Altering this number to reflect an earlier or later seasonal birth (200 or 300 d) did not affect disease model outcomes (data not shown). Within the hibernaculum, density-dependent fungal growth in the sediments continued year-round until the carrying capacity of the cave sediment was reached,

TABLE 2. The simulated survival of bat populations and environmental *Pseudogymnoascus destructans* (*Pd*) following a white-nose syndrome outbreak.

	Hibernation length					
	150 d	175 d	200 d	150 d	175 d	200 d
Sediment	No summer recovery			With summer recovery		
Myotis lucifugus colony size (% of original population)						
No growth	46.1	0[a]	0[b]	96.7	96.7	96.7
Stream sand	46.1	0[a]	0[b]	96.3	94.3	82.6
Stream gravel	43.1	0[a]	0[b]	90.6	77.1	34.7
Entrance sand	39.9	0[a]	0[b]	80.6	45.3	0.89
Clay	35.0	0[c]	0[b]	52.7	0.5	0.2
Flood debris	23.1	0[d]	0[e]	31.3	0[b]	0[e]
Persistence of *Pd* within cave sediments (yr)						
No growth	100	63.31	16.41	3.87	4.35	4.87
Stream sand	100	100	100	100	100	100
Stream gravel	100	100	100	100	100	100
Entrance sand	100	100	100	100	100	100
Clay	100	100	100	100	100	100
Flood debris	100	100	100	100	100	100

[a] Rate of colony extinction≤60 yr.
[b] Rate of colony extinction<20 yr.
[c] Rate of colony extinction<40 yr.
[d] Rate of colony extinction<30 yr.
[e] Rate of colony extinction<10 yr.

while spores were shed at a linear rate by infected bats:

$$Z_{t+1}=\beta_{br}\,Y_{\inf,t}+Z_t M\left(1-\frac{Z_t}{K_Z}\right)10^{\beta_{xr}} - Z_t 10^{-\mu_{Pd}} \quad (7)$$

where Z_t is the *Pd* subsidy (initial values: $Z_0=0$ or 1 CFU) at time t, β_{br} is the shed rate from live infectious bats (estimated at 100 CFUs/infected bat per day), β_{xr} is the empirical *Pd* growth rate (Table 1), and μ_{Pd} is the rate of *Pd* loss for a given sediment (Table 1). These growth parameters were generated under laboratory conditions and may therefore differ from the growth of *Pd* in natural settings.

To examine the role of hibernation season length on bat colony survival, we varied the length of this season from 150 to 200 d. In the absence of environmental *Pd* growth, WNS progressed through the bat colony via bat-to-bat transfer (Fig. 5A), and spore shedding led to the accumulation of environmental *Pd* above the infection threshold (10^6 spores per bat), which declined each season after hibernation when the bats departed (Fig. 5A). In the absence of environmental *Pd* growth, 100% mortality occurred at 60.4 yr for a 175-d hibernation season and 13.4 yr for a 200-d season (Table 2). When this season lasted 150 d, the bats persisted at a greatly reduced colony size under all *Pd* growth conditions (data not shown). The persistence of *Pd* on bats through the summer is unknown; histologic assays suggest that bats clear the fungus, while PCR-based assays suggest that infected bats may carry *Pd* spores into the next hibernation season (Meteyer et al. 2009, 2011). We simulated full clearance of *Pd* from bats in the summer and found that while it led to bat colony survival under most conditions, in high-nutrient environments, *Pd* growth actually accelerated the extirpation rate (Fig. 5B and Table 2).

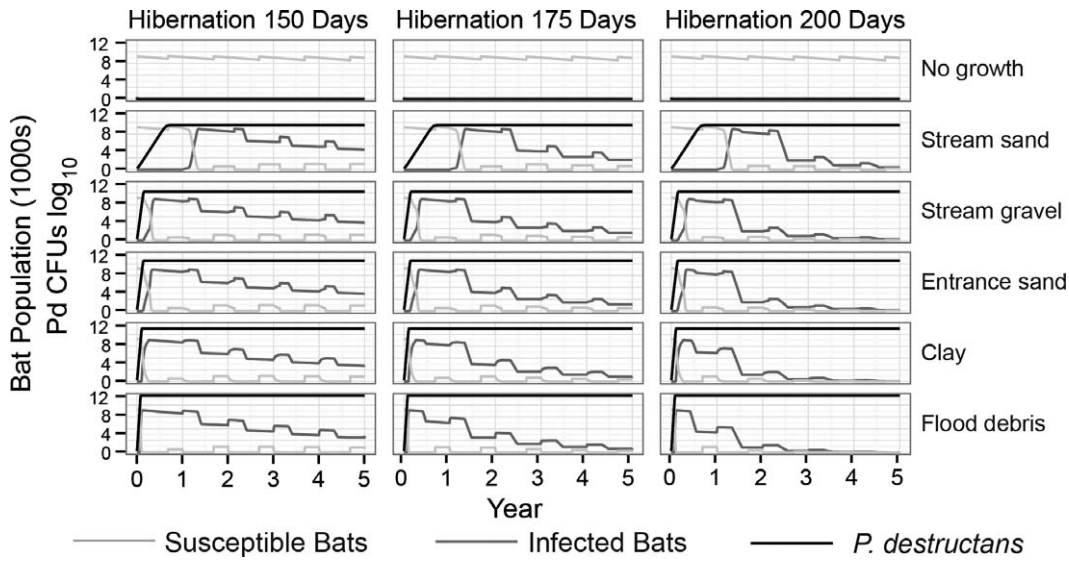

FIGURE 6. The influence of vector-transported *Pseudogymnoascus destructans* (*Pd*) on white-nose syndrome disease outcome and colony extirpation. The simulations of Figure 5A are repeated; however, in this scenario, a single *Pd* spore is introduced directly into the hibernaculum (simulating an introduced fomite). When environmental growth is zero ($\beta_{xr}=0$), *Pd* colony-forming unit (CFU) density within the sediments remains below the infection threshold for bats, and no animals are infected. When growth is permitted, bats quickly become infected, leading to collapse of the bat colony under the longer hibernation periods; extinction is measured as the complete loss of all individuals (Table 2).

In these initial simulations, we assumed that *Pd* introduction occurred via a WNS-infected bat; however, because the role that humans could play in *Pd* transport is not understood, we also simulated the impact of *Pd* introduction via a fomite (Fig. 6). When no environmental *Pd* growth was allowed, introduced *Pd* did not accumulate within the environment and remained below the infection threshold (Fig. 6); the saw-like pattern observed in the bat colony is due to natural mortality, with numbers rebounding annually through reproduction (Fig. 6). When *Pd* growth was allowed in each of the five sediments, *Pd* accumulated above the infection threshold (β_{xb}), and WNS disease progression was observed (Fig. 6). The progression from *Pd* introduction to WNS-associated mortality in nonrecovering bats occurred at all levels of fungal growth, with flood debris producing the highest bat mortality (Fig. 6 and Table 3).

Finally, we examined the effect of various levels of environmental *Pd* growth on colony survival. In the absence of environmental growth, the pathogen persisted for only 3 yr beyond the loss of the bats (Table 2); however, when growth was modeled at the in vitro rates of our experiments (Table 1), the fungus persisted for the full length of the simulations (100 yr), even in the most nutrient-limited sediments (Table 2). In the natural environment, biotic and abiotic factors (such as temperature, humidity, and microbial competition) could suppress *Pd* growth below that measured in our assays (Langwig et al. 2012). We therefore modeled how such suppression of *Pd* growth could affect WNS progression (Table 3). The results suggest that when *Pd* persists through the summer on bats, and environmental *Pd* growth is suppressed 10-fold, bat colony survival is dependent upon the amount of available carbon in the sediment to support *Pd*, evidenced by the survival of the colony with the stream sand and the extirpation of the colonies with the higher-carbon sediments (Table 3).

TABLE 3. Simulations on the subsistence of a *Myotis lucifugus* colony (% survival of original colony) after a white-nose syndrome outbreak in various *Pseudogymnoascus destructans* (*Pd*) growth rate scenarios.

Hibernation duration	Sediment	Comparative *Pd* growth rate suppression							
		10^3	10^2	10^1	None	10^3	10^2	10^1	None
		No summer recovery in bats				Full summer recovery in bats			
175 d	No growth	95.6	95.6	95.6	95.6	95.6	95.6	95.6	95.6
	Stream sand	95.6	95.6	95.6	0[a]	95.6	95.6	95.6	93.3
	Stream gravel	95.6	95.6	0[b]	0[a]	95.6	95.6	94.5	74.8
	Entrance sand	95.6	0[b]	0[b]	0[a]	95.6	95.6	89.7	45.2
	Clay	95.6	95.6	0[a]	0[c]	95.6	95.6	77.9	0.5
	Flood debris	95.6	95.6	0[a]	0[d]	95.6	95.6	1.3	0[e]
200 d	No growth	95.6	95.6	95.6	95.6	95.6	95.6	95.6	95.6
	Stream sand	95.6	95.6	95.6	0[e]	95.6	95.6	95.6	81.8
	Stream gravel	95.6	95.6	0[e]	0[e]	95.6	95.6	87.5	34.7
	Entrance sand	95.6	0[c]	0[e]	0[e]	95.6	94.1	70.5	0.9
	Clay	95.6	95.6	0[e]	0[e]	95.6	95.6	34.7	0.2
	Flood debris	95.6	95.6	0[e]	0[f]	95.6	95.6	0.3	0[f]

[a] Rate of colony extinction≤60 yr.

[b] Rate of colony extinction≤80 yr.

[c] Rate of colony extinction≤40 yr.

[d] Rate of colony extinction≤30 yr.

[e] Rate of colony extinction≤20 yr.

[f] Rate of colony extinction≤10 yr.

A 100-fold suppression in *Pd* growth leads to the survival of the bat colony under more conditions; however, extinction is still observed in entrance sand (Table 3), emphasizing the possible contribution of environmental growth to disease progression. Summer elimination of *Pd* from bat skin decreases the likelihood of extirpation in most scenarios, but it can accelerate extirpation in others (Table 3), suggesting a complex interaction between environmental *Pd* growth and bat survival.

DISCUSSION

We examined environmental growth of *Pd* in various simulated sediments and evaluated the effect such growth would have on WNS outcomes in hibernating *M. lucifugus* colonies. For practical reasons, we focused on sediments from one of the most cave-rich geologic units in the US: the Ste. Genevieve Limestone Formation, which houses hibernacula for a variety of bat species through Kentucky, Illinois, and Missouri. We demonstrated growth of *Pd* under all conditions tested, with growth influenced by geochemistry and the amount of available organic carbon (Fig. 1 and Table 1). Flood debris consisting of leafy detritus gave the greatest *Pd* growth (β_{xr}) per milligram of organic carbon (Table 1), suggesting that cellulose-rich material may best support *Pd* growth, in agreement with our previous findings (Reynolds and Barton 2014). The absolute fungal load of *Pd* (K_z) also appears to depend on the total amount of organic carbon available for saprotrophic growth (Figs. 2, 3 and Table 1). To assess the influences such growth would have on hibernating *M. lucifugus* colonies, we used a mathematic (SIS) model to examine bat colony survival (Figs. 1, 5, and 6).

The validity of such a mathematic approach depends on assumed parameters that have yet to be established for WNS disease progression, such as how many *Pd* spores constitute a minimum infectious dose; we assume a conservative 10^6 spores, extrapolated from the work of Lorch et al. (2011). The social interactions of bats during hibernation also make animal-pathogen transmission dynamics difficult to

estimate (McCallum et al. 2009). We therefore chose a conservative transmission coefficient (β_{xb}) of one bat per infected bat per day, although the increased arousal movement in bats as a result of WNS-infection would lead to a far greater number of daily contacts (Wilcox et al. 2014). Thus, using what we consider to be a conservative approach, we used a mathematic model to examine how varying the hibernation season from 150 to 200 d influences disease outcome (Fig. 5). In the experiments that confirmed *Pd* as the etiologic agent of WNS, almost 50% of *Pd*-inoculated bats survived the 102-d duration of the infection (Lorch et al. 2011); however, this was a small set of bats under caged laboratory conditions. From this result, we estimate that 120 d are required for WNS-associated mortality, potentially linking the severity of the WNS epidemic to hibernation length (Lorch et al. 2011).

The hibernation season length depends on the length of winter; bats in northern latitudes may enter hibernation as early as September and emerge in late April or early May, which can exceed 240 d (Quay 1976). Our simulations (Fig. 5) indicate that southern populations may be shielded from sharp WNS declines by a short hibernation season, but they could experience a spike in bat mortality in the event of a long winter. Simulations of WNS impact on bat evaporative water loss also suggested a strong effect of hibernation length on survival (Ehlman et al. 2013). To test this possibility, it will be interesting to observe the impact the long, cold winter of 2013–14 had on southern US bat populations. Although high mortalities have not been observed in southern hibernacula (Holliday 2012), questions remain regarding the interaction of climate, *Pd* growth rates, and WNS-induced mortality, which are worthy of additional study.

Our mathematic simulations also revealed other factors that could influence disease outcome, including the complete loss of *Pd* on bats during the summer, the amount of organic carbon for *Pd* growth, and *Pd* growth suppression. While it is easy to recognize that higher TOC can lead to higher levels of *Pd* spores, the confounding impact of bats clearing *Pd* in the summer is more difficult to discern, particularly in the case of *Pd* growth suppression (Table 2). The SIS model we employed uses a density-dependent function for the bat-to-bat transfer of *Pd*. In such a model, summer elimination of *Pd* returns all individuals to a susceptible state before the next hibernation season; however, in hibernacula containing the highest fungal growth, returning animals may enter a highly infectious environment. The healthy nature of these returning bats means that a larger colony survives to 120 d, allowing an increased rate of bat-to-bat *Pd* transfer up until this time. Thus, while bat-to-bat transfer appears to play the strongest role in WNS disease ecology, the environmental growth of *Pd* can still influence the rate of WNS disease progression within the colony.

Critically, other than anecdotal evidence of naïve bats succumbing to *Pd* from the environment, there are no published data documenting environment-to-bat or human-vectored transfer of *Pd* to naïve bats. Bat-to-bat transfer is clearly critical to the epidemic, given the movement of WNS along bat migration routes (Reynolds and Barton 2013), and the strong correlation between new outbreaks and proximity to infected hibernacula (Thogmartin et al. 2012). In our model, even in the absence of environmental growth, the introduction of *Pd* from an infected bat led to WNS infection and colony extirpation (Fig. 5), although we were able to demonstrate colony extirpation rates similar to real-world bat colony collapse (within 3–4 yr of introduction *Pd*) only when environmental growth of *Pd* occurred (Tables 2 and 3). Nonetheless, we only measured colony collapse based on the WNS-associated extinction of the entire colony; it is possible that, even in the absence of environmental *Pd*

growth, stochastic and Allee affects could result in the collapse of a colony well before the loss of all animals from WNS.

A great deal of effort has been made to limit the human-vectored transport of *Pd* by both cave researchers and recreational visitors (Shelley et al. 2013). This work demonstrates that the inadvertent introduction of spores into the environment could allow a WNS epidemic, reemphasizing the need for effective decontamination efforts (Shelley et al. 2013). Further, given that our simulations suggest that environmental growth can allow *Pd* to subsist for decades in infected hibernacula, any attempt at reintroduction of uninfected bats to contaminated sites would likely end in the extirpation of the reintroduced animals. This work also suggests that the removal of decaying organic material from hibernacula could limit the contribution of environmental *Pd* growth only under certain conditions. Finally, the model prediction that summer elimination of *Pd* from bats may actually accelerate WNS progression reveals that much research remains to be done in examining the complexities of the host-pathogen-environment relationship within WNS.

ACKNOWLEDGMENTS

We thank Paula Federico for her invaluable suggestions and review of our manuscript, DeeAnn Reeder for critical input on bat behavior, physiology, and bat colony dynamics, Tim Williams and Beth Cortright for assistance in fieldwork, Tom Quick for assistance with SEM-EDAX, and Kelsey Njus for laboratory assistance. Funding for this study was provided from the US Fish and Wildlife Service to H.A.B.

SUPPLEMENTARY MATERIAL

Supplementary material for this article is online at http://dx.doi.org/10.7589/2014-06-157.

LITERATURE CITED

Anderson RM. 1991. Discussion: The Kermack-McKendrick epidemic threshold theorem. *Bull Math Biol* 53:3–32.

Anderson RM, May RM. 1981. The population dynamics of microparasites and their invertebrate hosts. *Phil Trans Royal Soc London B Biol Sci* 291:451–524.

Boyer DG, Pasquarell C. 1996. Agricultural land use effects on nitrate concentrations in a mature karst aquifer. *J Am Water Res Asso* 32:565–573.

de Castro F, Bolker B. 2005. Mechanisms of disease-induced extinction. *Ecol Lett* 8:117–126.

Ehlman SM, Cox JJ, Crowly PH. 2013. Evaporative water loss, spatial distributions, and survival in white-nose-syndrome–affected little brown myotis: A model. *J Mammalogy* 94:572–583.

Fisher MC, Henk DA, Briggs CJ, Brownstein JS, Madoff LC, Mccraw SL, Gurr SJ. 2012. Emerging fungal threats to animal plant and ecosystem health. *Nature* 484:186–194.

Frick WF, Pollock JF, Hicks AC, Langwig KE, Reynolds S, Turner GG, Butchkoski CM, Kunz TH. 2010a. An emerging disease causes regional population collapse of a common North American bat species. *Science* 329:670–682.

Frick WF, Reynolds DS, Kunz TH. 2010b. Influence of climate and reproductive timing on demography of little brown myotis *Myotis lucifugus*. *J Animal Ecol* 79:128–136.

Gargas A, Trest MT, Christensen M, Volk TJ, Blehert DS. 2009. *Geomyces destructans* sp. nov. associated with bat white-nose syndrome. *Mycotaxon* 108:147–154.

Godfray HCJ, Briggs CJ, Barlow ND, O'Callaghan M, Glare TR, Jackson TA. 1999. A model of insect-pathogen dynamics in which a pathogenic bacterium can also reproduce saprophytically. *Proc R Soc Lond B* 266:233–240.

Holliday C. 2012. *White-nose syndrome disease surveillance and bat population monitoring report: A report of the Tennessee WNS response cooperators*. The Tennessee Chapter of the Nature Conservancy, Nashville, Tennessee, 10 pp.

Johnson LJ, Miller AN, McCleery RA, Mcclanahan R, Kath JA, Lueschow S, Porras-Alfaro A. 2013. Psychrophilic and psychrotolerant fungi on bats: *Geomyces* a common fungus on bat wings prior to the arrival of white-nose syndrome. *Appl Env Microbiology* 79:5465–5471.

Keeling MJ, Rohani P. 2008. *Modeling infectious diseases in humans and animals*. Princeton University Press, Princeton, New Jersey, 408 pp.

Keen R, Hitchcok HB. 1980. Survival and longevity of the little brown bat (*Myotis lucifugus*) in southeastern Ontario. *J Mammalogy* 61:1–7.

Krochmal AR, Sparks DW. 2007. Timing of birth and estimation of age of juvenile *Myotis septentrionalis* and *Myotis lucifugus* in west-central Indiana. *J Mammalogy* 88:649–656.

Langwig KE, Frick WF, Bried JT, Hicks AC, Kunz TH, Kilpatrick AM. 2012. Sociality, density-dependence and microclimates determine the

persistence of populations suffering from a novel fungal disease, white-nose syndrome. *Ecol Lett* 15:1050–1057.

Leconte JE. 1831. *The animal kingdom arranged in conformity with its organization,* translated by H. McMurtrie. G. & C. & H. Carville, New York, New York, 431 pp.

Lindner DL, Gargas A, Lorch J, Banik MT, Glaeser J, Kunz TH, Blehert DS. 2011. DNA-based detection of the fungal pathogen *Geomyces destructans* in soil from bat hibernacula. *Mycologia* 103:241–246.

Lorch JM, Lindner DL, Gargas A, Muller LK, Minnis AM, Blehert DS. 2013a. A culture-based survey of fungi in soil from bat hibernacula in the eastern United States and its implications for detection of *Geomyces destructans*, the causal agent of bat white-nose syndrome. *Mycologia* 105:237–252.

Lorch JM, Meteyer CU, Behr MJ, Boyles JG, Cryan PM, Hicks AC, Ballmann AE, Coleman JT, Redell DN, Reeder DM, et al. 2011. Experimental infection of bats with *Geomyces destructans* causes white-nose syndrome. *Nature* 480: 376–378.

Lorch JM, Muller LK, Russell RE, O'Connor M, Lindner DL, Blehert DS. 2013b. Distribution and environmental persistence of the causative agent of white-nose syndrome, *Geomyces destructans*, in bat hibernacula of the eastern United States. *Appl Env Microbiol* 79:1293–1301.

Maresca B, Kobayashi Gs. 1989. Dimorphism in *Histoplasma capsulatum*: A model for the cell differentiation in pathogenic fungi. *Microbiol Mol Biology Rev* 53:186–209.

McCallum H, Jones M, Hawkins C, Hamede R, Lachish S, Sinn DL, Beeton N, Lazenby B. 2009. Transmission dynamics of Tasmanian devil facial tumor disease may lead to disease-induced extinction. *Ecology* 90:3379–3392.

Meteyer CU, Buckles EL, Blehert DS, Hicks AC, Green DE, Shearn-Bochsler V, Thomas NJ, Gargas A, Behr MJ. 2009. Histopathologic criteria to confirm white-nose syndrome in bats. *J Vet Diagn Invest* 21:411–414.

Meteyer CU, Valent M, Kashmer J, Buckles EL, Lorch JM, Blehert DS, Lollar A, Berndt D, Wheeler E, White CL, et al. 2011. Recovery of little brown bats (*Myotis lucifugus*) from natural infection with *Geomyces destructans*, white-nose syndrome. *J Wildl Dis* 47:618–626.

Minnis AM, Lindner DL. 2013. Phylogenetic evaluation of *Geomyces* and allies reveals no close relatives of *Pseudogymnoascus destructans*, comb. nov., in bat hibernacula of eastern North America. *Mycological Res* 117:638–649.

Mitchell KM, Churcher TS, Garner TWJ, Fisher MC. 2008. Persistence of the emerging pathogen *Batrachochytrium dendrobatidis* outside the amphibian host greatly increases the probability of host extinction. *Proc R Soc B* 275:329–334.

Quay WB. 1976. Seasonal cycle and physiological correlates of pinealocyte nuclear and nucleolar diameters in the bats, *Myotis lucifugus* and *Myotis sodalis*. *Gen Comp Endocrin* 29:369–375.

R Development Core Team. 2012. *R: A language and environment for statistical computing*. R Foundation for Statistical Computing, Vienna, Austria, http://www.R-project.org. Accessed January 2014.

Raudabaugh DB, Miller AN. 2013. Nutritional capability of and substrate suitability for *Pseudogymnoascus destructans*, the causal agent of bat white-nose syndrome. *PLoS One* 8:e78300.

Reynolds HT, Barton HA. 2013. White-nose syndrome: Human activity in the emergence of an extirpating mycosis. *Microbiol Spectr* 1:1–11.

Reynolds HT, Barton HA. 2014. Comparison of the white-nose syndrome agent *Pseudogymnoascus destructans* to cave-dwelling relatives suggests reduced saprophytic enzyme activity. *PLoS One* 9:e86437.

Shelley V, Kaiser S, Shelley E, Williams T, Kramer M, Haman KH, Keel MK, Barton HA. 2013. Evaluation of strategies for the decontamination of equipment for *Geomyces destructans,* the causative agent of white-nose syndrome. *J Cave Karst Stud* 75:1–10.

Smyth C, Schlesinger S, Overton BE, Butchkoski C. 2013. The alternative host hypothesis and potential virulence genes in *Geomyces destructans*. *Bat Res News* 54:17–24.

Thogmartin WE, King RA, Szymanski JA, Pruitt L. 2012. Space-time models for a panzootic in bats, with a focus on the endangered Indiana bat. *J Wildl Dis* 48:876–887.

Turner GG, Reeder DM, Coleman JTH. 2011. A five-year assessment of mortality and geographic spread of white-nose syndrome in North American bats and a look at the future. *Bat Res News* 52:13–27.

Vanderwolf KJ, McAlpine DF, Malloch D, Forbes GJ. 2013. Ectomycota associated with hibernating bats in eastern Canadian caves prior to the emergence of white-nose syndrome. *Northeastern Nat* 20:115–130.

Verant ML, Boyles JG, Waldrep W Jr, Wibbelt G, Blehert DS. 2012. Temperature-dependent growth of *Geomyces destructans*, the fungus that causes bat white-nose syndrome. *PLoS One* 7:e46280.

Wilcox A, Warnecke L, Turner JM, McGuire LP, Jameson JW, Misra V, Bollinger TK, Willis CK. 2014. Behavior of hibernating little brown bats experimentally inoculated with the pathogen that causes white-nose syndrome. *Anim Behav* 88:157–164.

Submitted for publication 23 June 2014.
Accepted 1 November 2014.